inorganics

MDPI

Article

Photoluminescent Coordination Polymers Based on Group 12 Metals and 1*H*-Indazole-6-Carboxylic Acid

Antonio A. García-Valdivia [1], Estitxu Echenique-Errandonea [2], Gloria B. Ramírez-Rodríguez [1], José M. Delgado-López [1], Belén Fernández [3], Sara Rojas [1], Javier Cepeda [2,*] and Antonio Rodríguez-Diéguez [1,*]

1 Departamento de Química Inorgánica, Facultad de Ciencias, Universidad de Granada, 18071 Granada, Spain; antonioandresgarval@correo.ugr.es (A.A.G.-V.); gloria@ugr.es (G.B.R.-R.); jmdl@ugr.es (J.M.D.-L.); srojas@ugr.es (S.R.)

2 Departamento de Química Aplicada, Facultad de Química, Universidad del País Vasco/Euskal Herriko Unibertsitatea (UPV/EHU), 20018 Donostia, Spain; estitxu.echenique@ehu.eus

3 Institute of Parasitology and Biomedicine "López-Neyra", CSIC, 18600 Granada, Spain; belenfernandez@ipb.csic.es

* Correspondence: javier.cepeda@ehu.es (J.C.); antonio5@ugr.es (A.R.-D.); Tel.: +34-943015409 (J.C.); +34-958248524 (A.R.-D.)

Abstract: Two new coordination polymers (CPs) based on Zn(II) and Cd(II) and 1*H*-indazole-6-carboxylic acid (H_2L) of general formulae $[Zn(L)(H_2O)]_n$ (**1**) and $[Cd_2(HL)_4]_n$ (**2**) have been synthesized and fully characterized by elemental analyses, Fourier transformed infrared spectroscopy and single crystal X-ray diffraction. The results indicate that compound **1** possesses double chains in its structure whereas **2** exhibits a 3D network. The intermolecular interactions, including hydrogen bonds, C–H···π and π···π stacking interactions, stabilize both crystal structures. Photoluminescence (PL) properties have shown that compounds **1** and **2** present similar emission spectra compared to the free-ligand. The emission spectra are also studied from the theoretical point of view by means of time-dependent density-functional theory (TD-DFT) calculations to confirm that ligand-centred π-π* electronic transitions govern emission of compound **1** and **2**. Finally, the PL properties are also studied in aqueous solution to explore the stability and emission capacity of the compounds.

Keywords: group 12 metals; 1*H*-indazole-6-carboxylic acid; coordination polymer; photoluminescence properties

Citation: García-Valdivia, A.A.; Echenique-Errandonea, E.; Ramírez-Rodríguez, G.B.; Delgado-López, J.M.; Fernández, B.; Rojas, S.; Cepeda, J.; Rodríguez-Diéguez, A. Photoluminescent Coordination Polymers Based on Group 12 Metals and 1*H*-Indazole-6-Carboxylic Acid. *Inorganics* **2021**, *9*, 20. https://doi.org/10.3390/inorganics9030020

Academic Editor: Andrea Rossin

Received: 16 January 2021
Accepted: 17 March 2021
Published: 22 March 2021

1. Introduction

The study of coordination polymers (CPs) and metal-organic frameworks (MOFs) is at the forefront of modern inorganic chemistry due to their broad range of potential applications, spanning from magnetism and luminescence, through catalysis and sensing, to gas separation and storage, and biomedicine [1,2]. Through an adequate selection of their building blocks (metal ions and organic ligands), CPs and MOFs can be designed to enhance a particular property [3–5]. It is well known that nitrogen-containing heterocycles are molecules commonly employed as ligands owing to not only their good coordination ability, but also pharmacological relevance, given that they are important scaffolds widely present in numerous commercially available drugs [6]. The most famous are diazepam, isoniazid, chlorpromazine, metronidazole, barbituric acid, captopril, chloroquinine, azidothymidine and anti-pyrine. As a result of their diverse biological activities, nitrogen heterocyclic compounds have always been attractive targets to develop new active compounds. This is the case for 1*H*-indazole-6-carboxylic acid (H_2L), a common moiety in the pharmaceutical industry [7]. Polysubstituted indazole-containing compounds furnished with different functional groups usually present significant pharmacological activities and serve as structural motifs in drug molecules (i.e., niraparib-anticancer drug, pazopanib-approved by the FDA for renal cell carcinoma, bendazac and benzydamine-antiinflamatory

drugs) [8]. From the structural point of view, indazole is an aromatic heterocyclic molecule with a benzene ring fused to a pyrazole ring [9]. It shows three tautomeric forms (Scheme 1) being tautomer **A** favoured over **B** and **C** due to its higher degree of aromaticity [10].

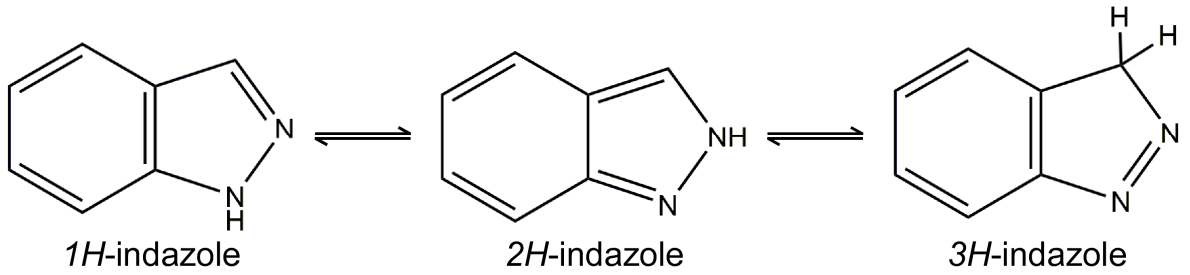

Scheme 1. Indazole tautomerism (**A**, **B**, and **C** from left to right).

H_2L is presented here as an ideal candidate to form CPs or MOFs as it possesses multiple coordination possibilities, not only derived from its carboxylate group, but also from its pyrazole function. Thus, a great variety of coordination modes are possible, according to similar ligands containing carboxylate and pyrazole chemical functions in crystallized complexes (Scheme 2). Until now, only one complex based on this ligand has been reported so far [11]. In that work, Kruger et al. described in detail four substituted indazole derivatives containing pyridine or carboxylic functionalities upon coordination with Cu(II) ions in solution and solid state. In the complex, 1*H*-indazole-6-carboxylate acts as a bridging ligand showing a tridentate coordination mode: the carboxylate group coordinates to two Cu(II) atoms in a *syn*,*syn* mode to establish a dimeric paddle-wheel shaped entity, whereas the non-protonated nitrogen atom of the pyrazole ring links to a third Cu(II) atom in a monodentate way (see the highlighted modes in Scheme 2). Aside from this work mainly focused on the description of a new compound, it should be pointed out that some Co(II)-based complexes with indazole derivatives have shown a capacity to bind to DNA [12].

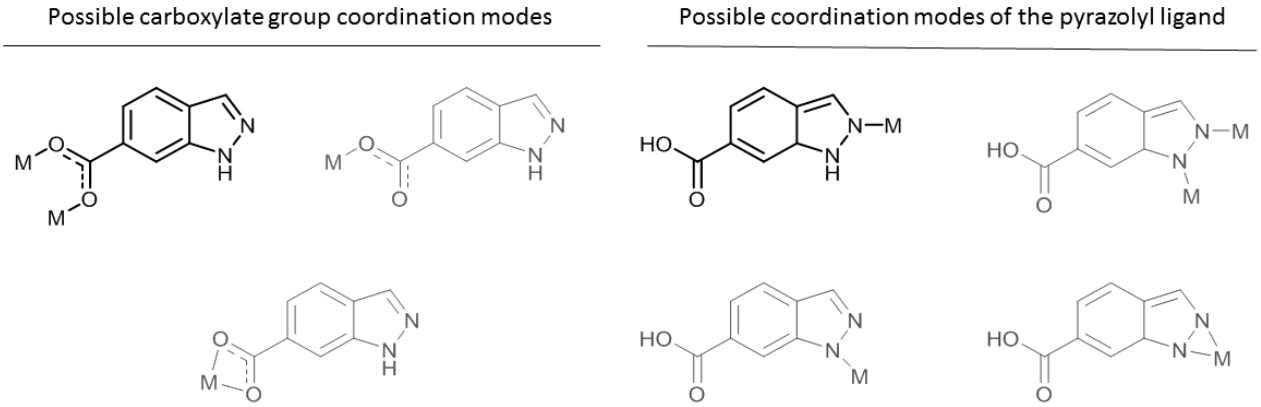

Scheme 2. Possible coordination modes of *1H*-indazole-6-caboxylate ligand. Note that only those two modes highlighted in black have been described in bibliography whereas the rest correspond to potential binding modes.

On the other hand, H_2L may also present interesting photoluminescence (PL) properties due to its aromatic nature and the presence of carboxylic groups, with potentially strong light absorption [13]. When these indazole-carboxylate ligands are coordinated to metal centres in the crystal structure of a CP, PL tends to be enhanced by means of the well-known crystal-induced luminescence effect [14]. Among others, metal ions from group 12 are particularly appropriate for their use in PL as they present a closed-shell electronic configuration in which d-d transitions cannot occur [15,16]. In fact, many CPs and MOFs formed by these metal ions have been reported during the last decade [17,18], some of which present not only strong and bright fluorescent emissions, but also long-lived phosphorescence that may be traced by the naked eye [19–21]. Moreover, the presence of these ions may also promote ligand-to-metal charge transfer (LMCT) as metal ions possess empty orbitals that can be populated in the excited state, and therefore the PL emission may be modulated with regard to the ligand-centred (LC) emissions [22,23]. Irrespective of the luminescence mechanism occurring in these systems, the interest for group 12-based compounds has increased given their potential application as not only lighting devices, but also as luminescence-based molecular detectors [24], thermometers [25] and anti-counterfeiting inks, among others [26]. Particularly for indazole derivatives playing as ligands, many Zn-/Cd-indazole complexes have already proved efficient luminescent CPs under UV irradiation [27].

Considering all the above, in this work we present the synthesis, structural characterisation and PL properties of two new coordination polymers based on group 12 metals and 1*H*-indazole-6-carboxylic acid of general formula $[Zn(L)(H_2O)]_n$ (**1**) and $[Cd_2(HL)_4]_n$ (**2**). Their emission characteristics have been studied both from the theoretical and experimental points of view, involving the measurements in the solid state as well as in aqueous medium.

2. Results and Discussion

The reaction of 1*H*-indazole-6-carboxylic acid gave rise to two compounds based on group 12 metals which exhibit a different structural dimensionality. In particular, the solvothermal reaction of the 1*H*-indazole-6-carboxylic acid ligand with zinc acetate salt ($Zn(CH_3COO)_2$) using a 1:2 molar ratio in a *N*,*N*-dimethylformamide/water (DMF/H_2O) mixture afforded a 1D CP, namely **1** (see Experimental Section for further details). Similarly, the use of cadmium acetate salt ($Cd(CH_3COO)_2$) salt in the synthesis, successfully led to a 3D MOF, namely **2**. This fact can be explained by the larger ion size of Cd(II), which may admit higher coordination numbers, involving the participation of additional ligands and increasing the metal-to-ligand connectivity.

2.1. Description of the Structures

2.1.1. Structural Description of $[Zn(L)(H_2O)]_n$ (**1**)

Compound **1** crystallizes in the $P2_1/n$ space group and consists of a double chain structure in which Zn(II) ions are bridged by nitrogen atoms of L^{2-} in a bidentate way, giving rise to a stable and in plane Zn_2N_4 dimeric core as a six membered ring (Figure 1).

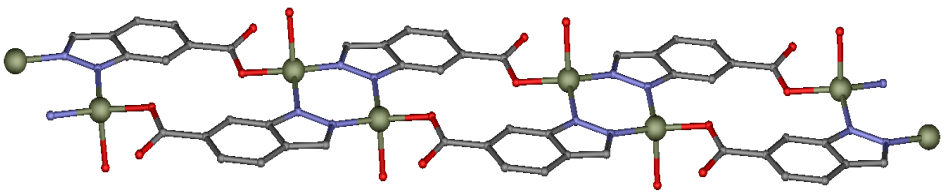

Figure 1. Representation of the 1D polymeric chain in which Zn_2N_4 planar six membered ring is observed (zinc, nitrogen, oxygen, and carbon are represented in green, blue, red, and grey, respectively; hydrogen atoms are omitted for clarity).

The Zn(II) ion is also coordinated to a carboxylate moiety of the indazole derivative ligand in a monodentate way, which extends the dimeric entity into infinite 1D chains running along the crystallographic [100] direction. The coordination sphere of Zn is completed by the coordination of a water molecule (see Table S1 in the ESI for further information about bond lengths and angles). The ZnN_2O_2 coordination sphere can be described as a tetrahedron, although Zn ions show a geometry close to an axially vacant trigonal bipyramid according to continuous-shape-measures (CShMs) using SHAPE software (Tables S2 and S3, in the ESI) [28].

The packing of the double chains is ruled by intermolecular interactions, among which hydrogen bonding interactions established between coordination water molecules and carboxylate oxygen atoms are to be highlighted (Figure 2). In particular, the coordinated water molecule is involved in hydrogen bonding interactions in which non-coordinated carboxylate oxygen atoms belonging to adjacent chains act as receptors. Additionally, the angle formed among neighbouring chains allows for the formation of C–H···π interactions between aromatic rings, reinforcing the stability of the supramolecular crystal building (see Figure S5 in the ESI).

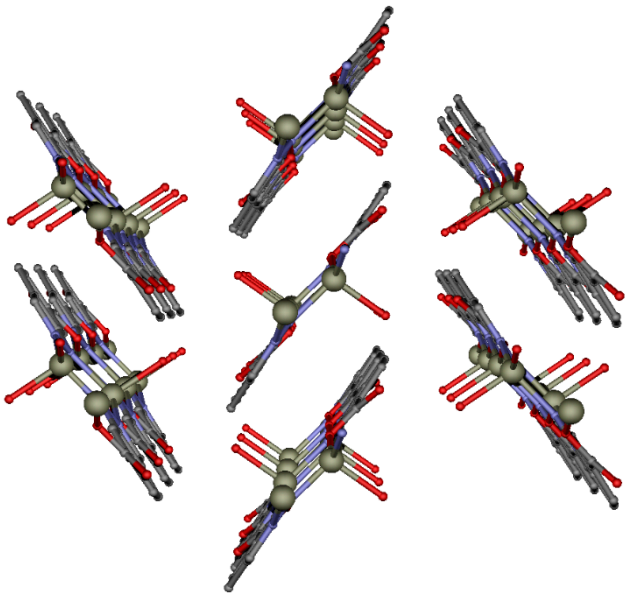

Figure 2. Perspective view of the chains of $[Zn(L)(H_2O)]_n$ packed in the framework (hydrogen atoms have been omitted for clarity).

2.1.2. Structural Description of $[Cd_2(HL)_4]_n$ (**2**)

Compound **2** crystallizes in the triclinic *P*-1 space group. The asymmetric unit contains two non-equivalent Cd(II) atoms and four ligand molecules. Each Cd(II) ion is connected to two monodentate indazole nitrogen atoms and four oxygen atoms of the carboxylate group of the ligand. Cd1 and Cd2 ions are doubly linked by ancillary *syn-anti* carboxylate moieties of 1-*H*-indazole-6-carboxylate ligands (namely A, C and D). However, the carboxylate group of B ligand presents a different coordination pattern, in which O1B connects in a monodentate way to both Cd1 and Cd2 atoms giving rise to alternating five and six membered rings (Figure 3, see also the view along *b* axis in Figure S6 in the ESI), whereas O2B atom remains unconnected to any metal centre.

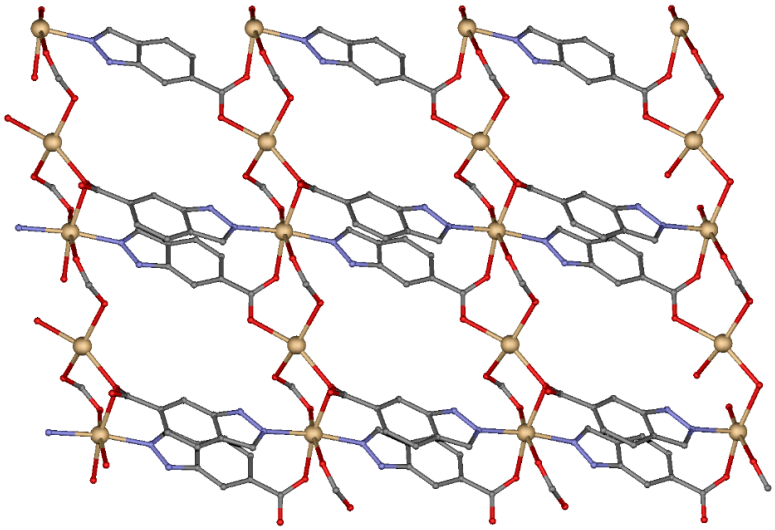

Figure 3. View of the coordination of Cd(II) ions to HL in compound **2** (cadmium, nitrogen, oxygen, and carbon are represented in dark-yellow, blue, red, and grey, respectively; hydrogen atoms have been omitted for clarity).

CShMs indicate that different ligand coordination modes affect the connectivity of the metal centres, which leads to the formation of a distinct crystal structure. When comparing **1** and **2** compounds, the coordination spheres of Cd1 and Cd2 are described as octahedra according to SHAPE measurements (Tables S2 and S3 in the SI). M···N2 distances are slightly shorter than in compound **1** (in the 1.969 and 2.293–2.316 Å ranges, respectively), similarly to the $M\cdots O1_{carboxylate}$ bond distances (between 1.935 and 2.320 Å, see Table S1 in the ESI). As a result, a 3D framework is obtained in the case of **2** by the further linkage of the carboxylate groups to Cd(II) atoms along a metal-carboxylate rod (Figure 4). Considering the connectivity of the metal ions and HL ligands, this framework may be described as a **5,6T24** topological network with the $(3^2.4^2.5^2.6^3.7)_2(3^2.4^4.5^4.6^2.7^3)$ point symbol, as previously observed in the MOF of $[Al_2(OH)_2(H_2O)_2(C_{10}O_8H_2)]$ or MIL-118A [29].

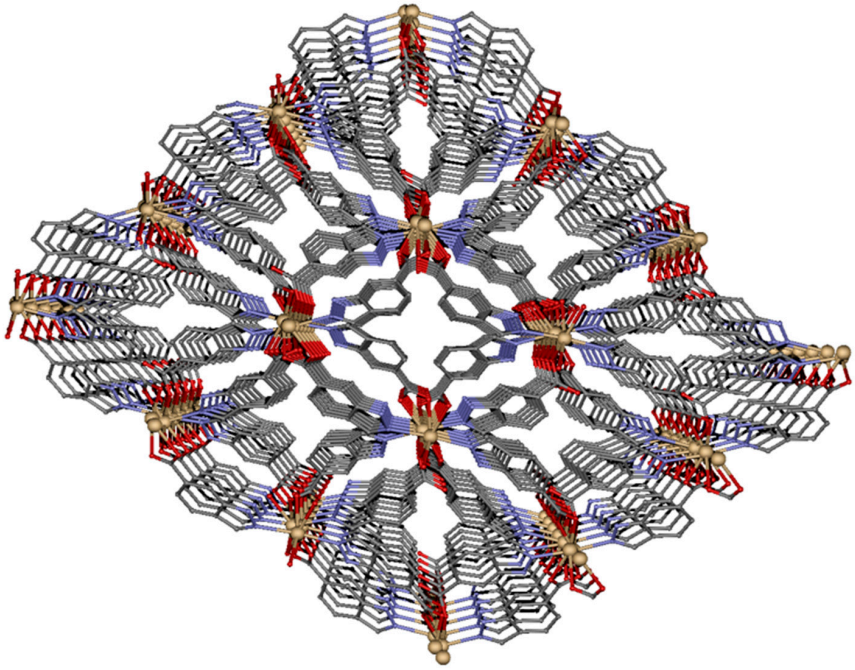

Figure 4. Perspective of 3D structure of compound **2** (hydrogen atoms have been omitted for clarity).

To end up with the structural description, it is worth mentioning that compound **2** presents some remarkable supramolecular interactions that reinforce its packing. Unlike with hydrogen bonding and C–H··· π interactions governing the crystal structure of **1**, **2** contains π···π stacking interactions. In particular, the aromatic rings of HL promote strong face-to-face contacts among the whole structure (see Figure S5 in the ESI).

2.2. Fourier Transformed Infrared (FTIR) Spectroscopy

The analysis of the FTIR spectra of **1** and **2** confirms the coordination of zinc(II) and cadmium(II) ions to the *N*-containing carboxylate ligand (Figure S1, see the ESI). FTIR spectra of both compounds confirmed a shift in the wavelengths in comparison to the pure linker, suggesting the formation of interactions between the linker and the metals. The main vibrations of 1*H*-indazole-6-caboxylic acid associated with the $\upsilon_{C=N}$ stretching vibration at 1633 cm^{-1}, and the asymmetric and symmetric vibrations of the carboxylate groups at 1683 and 1423 cm^{-1} are shifted when compared with the spectra of **1** and **2**. The bands found at 1537 and 1589 cm^{-1} for complex **1** and **2**, respectively, are attributed to the $\upsilon_{C=N}$ stretching vibration of the indazole ring [30]. Moreover, the strong absorption peak observed at 1558 and 1402 cm^{-1} for **1**, and 1541 and 1411 cm^{-1} for **2**, respectively, revealed the asymmetric and symmetric vibrations of the carboxylic groups [31]. Finally, the strong broad band in the range of 3317–3086 cm^{-1} was assigned to the O–H stretching vibration of the coordinated water molecule in complex **1** [32].

2.3. Luminescence Properties

As previously mentioned, complexes consisting of metal ions with d^{10} electronic configuration are known to yield strong PL emissions. The completely filled d-orbitals disable ligand field d-d transitions, eliminating fluorescence quenching and allowing the occurrence of PL [14]. Thus, the development of d^{10}-based compounds is interesting for photochemical, electroluminescence and sensing applications [17,33]. The extended aromaticity of the 1*H*-indazole-6-carboxylate ligand coordinated to Zn(II) and Cd(II) atoms suggests the existence of emissive properties of **1** and **2**. The emission of these compounds are found to be similar to ligand emission, which may stem from the ligand-centred π–π^* electronic transitions, as shown in Figure 5. Consequently, it can be suggested that the highly conjugated 1*H*-indazole-6-caboxylate ligand is the main part contributing to the emission [34]. An intense broad band at 350–450 nm dominates the emission spectra of all compounds upon 325 nm excitation (in view of the maxima found in the excitation spectra), among which the maxima at 362 and 388 nm, 363 and 381 nm, and 363 and 391 nm can be distinguished for the ligand, and compounds **1** and **2**, respectively; which imbues all compounds with blue emission. The similar emission band of **2** and the free ligand must be attributed to the fact that **2** possesses the protonated form of the ligand (HL^-) whereas it is completely deprotonated (L^{2-}) in **1**. In a comparative scale, the ligand spectrum shows two well-defined maxima (not that easily identified for the compounds) and relatively higher intensity (Figure S2, SI). It is worth noticing that the observed luminescence resembles to that shown by other previously reported CPs containing other isomers of indazole-carboxylates [35,36].

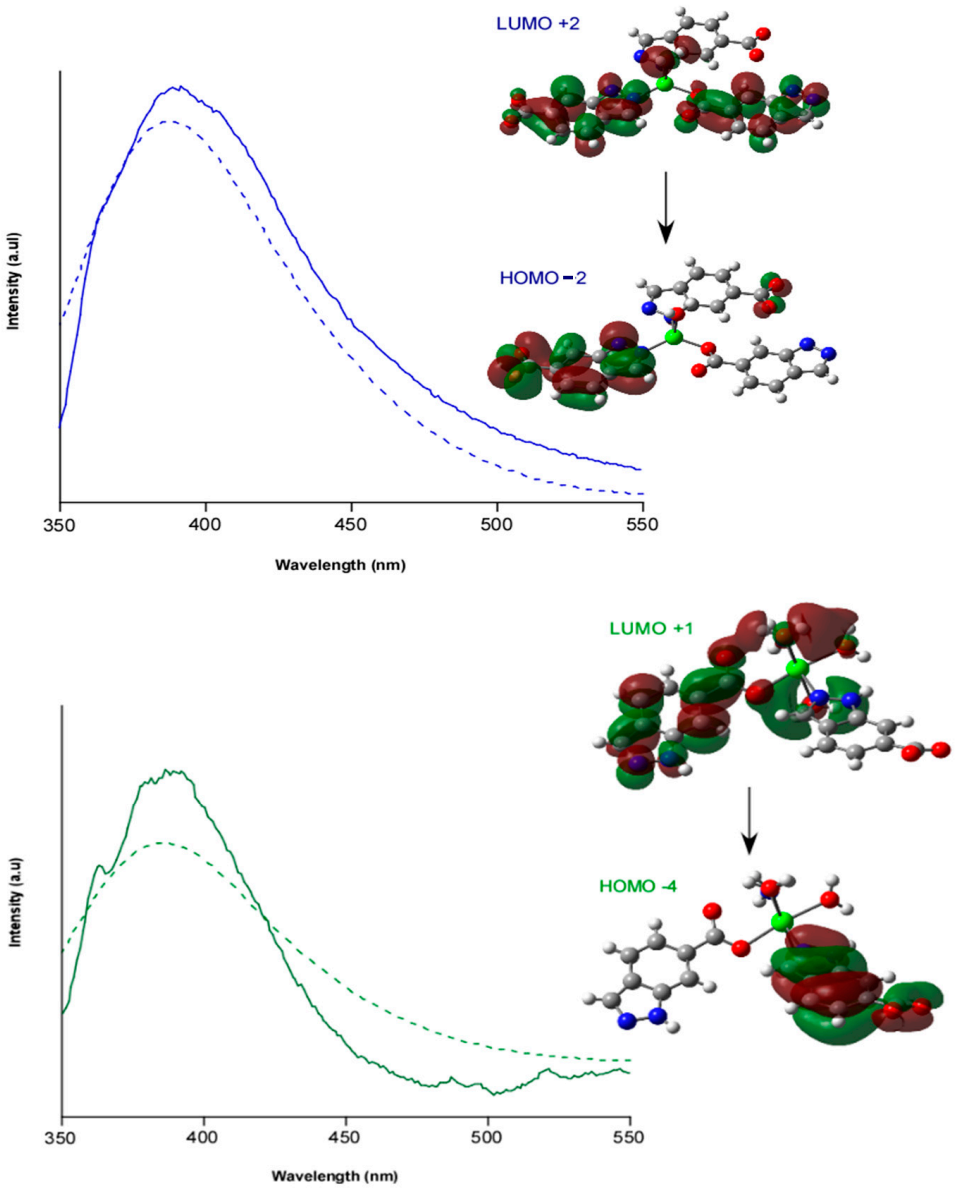

Figure 5. Room temperature Time-dependent density-functional theory (TD-DFT) computed (dashed lines) and experimental (solid line) photoluminescence emission under λ_{ex} = 325 nm of compounds **1** (blue-up) and **2** (green-down). The insets show the most representative molecular orbitals involved in the electronic transitions.

In order to get a deeper insight into the emission mechanism, TD-DFT calculations were performed on suitable models of compounds **1** and **2**. The calculated spectra reproduce fairly well the experimental ones, indicating that the process is driven by singlet transitions occurring between the molecular orbitals shown in Figure 5. In both cases, the electron density in HOMO orbitals, HOMO-2 and HOMO-4 for compound **1** and **2**, respectively, extend over the bonds over the whole ligand molecule (signifying a π orbital) whereas LUMO orbitals, LUMO+2 and LUMO+1 for compound **1** and **2**, respectively, feature a π* character. Therefore, it can be stated that the transitions involved in the photoluminescence of compound **1** and **2** are mainly of π*←π nature induced by ligand centred emission.

Inspired by the potential biomedical properties of the ligand on the basis of its similar structure to other indazole derivatives [7,8], we studied the stability and fluorescence

performance of these compounds in aqueous media in order to explore their performance as luminescent probes. First, the stability of both compounds was confirmed by recording UV-Vis absorption spectra on aqueous solutions of both compounds immediately after their solution and also after 24 h (see Figure S7 in the ESI). These spectra show the presence of three main absorption bands (sited at ca. 215, 265 and in the 340 nm for **1** and 220, 265 and 305 nm for **2**), corresponding to intraligand and/or ligand-to-metal charge transfers occurring in the complexes. It is worth noticing that these bands are in good agreement with the experimental and TD-DFT computed excitation bands, finding only slight shifts that may be attributed to the different media in which the spectra are recorded (water for UV-Vis and solid state for excitation spectra). Moreover, these solutions were also employed to measure the PL emission spectra of both compounds. As observed in Figure S4, the emission spectra acquired in this medium do not significantly differ from those measured in solid state but for a drop in the intensity of the signal, which is an expected behaviour given that the capacity of this solvent to quench the PL is a largely reported effect [37]. All these results suggest that these new compounds could show potential activity as luminescent probes in some particular biological media (i.e., as biosensor), a fact that *a priori* excludes most of biological tissues owing to their low transparency (high light absorption capacity) to the blue emission (λ_{em} = 350–450 nm) shown by these compounds.

3. Materials and Methods

3.1. Materials and Physical Measurements

All the reagents were purchased commercially and used without any previous purification. Elemental analysis (C, H and N) were carried out at the Centro de Instrumentación Científica (University of Granada) on a Fisons-Carlo Erba analyzer model EA 1108 (Thermo Scientific, Waltham, MA, USA). FTIR spectra (400–4000 cm^{-1}) were recorded on a Nicolet FT-IR 6700 spectrometer (Thermo Scientific, Madrid, Spain) in KBr pellets.

*3.2. Synthesis of $[Zn(L)(H_2O)]_n$ (**1**)*

0.010 g (0.006 mmol) of 1*H*-indazole-6-carboxylic acid (H_2L) was dissolved in 0.5 mL of DMF. Then, 0.5 mL of water was added to the ligand solution. In a separate vial, 0.0134 g (0.03 mmol) of $Zn(CH_3COO)_2$ was dissolved in 0.5 mL of water. Similarly, once metal salt was dissolved, 0.5 mL DMF were added to the solution. Metal solution was added dropwise to the ligand solution, and the resulting colourless mixture was placed in a closed glass vessel and heated in an oven at 100 °C for 24 h. X-ray quality crystals of **1** were obtained during heating process under autogenous pressure and washed with water. Yield: 64% based on Zn. Anal Calcd. for $C_8H_4N_2O_3Zn$: C, 39.46; H, 2.48; N, 11.50. Found: C, 39.39; H, 2,41; N, 11.59. In addition to the elemental analyses, the purity of all the samples was checked by FT-IR spectra.

*3.3. Synthesis of $[Cd_2(HL)_4]_n$ (**2**)*

The same synthetic procedure was carried out to obtain complex **2**, by replacing $Zn(CH_3COO)_2$ by 0.01651 g (0.03 mmol) of $Cd(CH_3COO)_2$. X-ray quality crystals were obtained and washed with water. Yield: 54% based on Cd. Anal Calcd. for $C_{32}H_{20}Cd_2N_8O_8$: C, 44.21; H, 2.32; N, 12.89. Found: C, 44.16; H, 2.29; N, 12.91. In addition to the elemental analyses, the purity of all the samples was checked by FT-IR spectra.

3.4. Crystallographic Refinement and Structure Solution

Single crystals of suitable dimensions were used for data collection. For compound **1** and **2**, diffraction intensities were recorded on a Bruker X8 APEX II and Bruker D8 Venture with a Photon detector (Bruker, Madrid, Spain) equipped with graphite monochromated MoKα radiation (λ = 0.71073 Å). The data reduction was performed with the APEX2 software [38] and corrected for absorption using SADABS [39]. In all cases, the structures were solved by direct methods and refined by full-matrix least-squares with SHELXL-2018 [40]. The main refinement parameters are listed in Table 1. Details of selected bond

lengths and angles are given in Table S2 in the ESI. CCDC reference numbers for the structures are 1,948,382 and 1,948,383 for Cd and Zn coordination polymers, respectively.

Table 1. Crystallographic data and structure refinement details of compounds **1** and **2**.

Compound	1	2
Formula	$C_8H_6N_2O_3Zn$	$C_{32}H_{20}Cd_2N_8O_8$
M_r (g mol^{-1})	243.52	869.36
Crystal system	monoclinic	triclinic
Space group	$P2_1/n$	P–1
Temperature (K)	100 (2)	100 (2)
a (Å)	9.774 (3)	8.7080 (4)
b (Å)	5.7633 (15)	9.0640 (3)
c (Å)	14.592 (4)	19.4510 (7)
α (°)	90	101.089 (1)
β (°)	95.626 (7)	90.961 (2)
λ (°)	90	98.063 (1)
V (Å^3)	818.0 (4)	1490.18 (1)
Z	4	2
ρ (g cm^{-3})	1.977	1.937
μ (mm^{-1})	2.979	1.497
Unique reflections	1035 (817)	7671 (5938)
R_{int}	0.1342	0.0722
GoF [a]	1.082	1.107
R_1 [b]/wR_2 [c] [I>2σ(I)]	0.0777/0.0535	0.0604/0.0352
R_1 [b]/wR_2 [c] [all data]	0.1075/0.0994	0.0823/0.0672
Largest difference in peak and hole (e Å^{-3})	0.635 and −0.0656	1.062 and −1.046

[a] $R_1 = S||F_o| - |F_c||/S|F_o|$. [b] Values in parentheses for reflections with $I > 2s(I)$. [c] $wR_2 = \{S[w(F_o^2 - F_c^2)^2] / S[w(F_o^2)^2]\}^{\frac{1}{2}}$; where w = $1/[\sigma^2(F_0^2) + (aP)^2 + bP]$ and P = $(\max(F_0^2,0) + 2Fc^2)/3$ with a = 0.0.0319 (**1**), 0.0380 (**2**) and b = 6.9969 (**1**).

3.5. Photophysical Measurements

UV-Vis absorption spectra were recorded on UV-2600 UV/vis Shimadzu spectrophotometer using polycrystalline samples of compounds **1** and **2**. PL measurements were carried out on crystalline samples at room temperature using a Varian Cary-Eclipse fluorescence spectrofluorometer equipped with a Xe discharge lamp (peak power equivalent to 75 kW), Czerny–Turner monochromators, and an R-928 photomultiplier tube. For the fluorescence measurements, the photomultiplier detector voltage was fixed at 600 V, and the excitation and emission slits were set at 5 and 2.5 nm, respectively. Phosphorescence spectra were recorded with a total decay time of 20 ms, delay time of 0.2 ms and gate time of 5.0 ms. The photomultiplier detector voltage was set at 800 V, and both excitation and emission slits were open to 10 nm.

4. Conclusions

The reaction between 1*H*-indazole-6-carboxylic acid ligand and Zn(II) or Cd(II) leads the formation of two new coordination polymers with different dimensionalities. Compound **1** possesses a double chain structure, whereas compound **2** exhibits a 3D structure. Emissive properties of both complexes have been studied demonstrating that their photoluminescent emission is driven by the ligand centred $\pi^*\leftarrow\pi$ transition. The similar luminescent properties between compound **2** and the linker may be consequence of the partially protonated HL^- ligand present in **2**. This work is pioneer in studying and comparing the luminescent properties of 1*H*-indazole-6-carboxylic acid (H_2L) and its complexes, which represent a common moiety in pharmaceutical industry. In this regard, novel materials based on this ligand are being developed in our laboratory using lanthanide ions to enhance their luminescent properties.

Supplementary Materials: The following are available online at https://www.mdpi.com/2304-6740/9/3/20/s1, Figure S1: Infrared spectra of the ligand and compounds **1** and **2**, Figure S2: Emission spectra of the ligand and compounds **1** and **2** under λ_{ex} = 325 nm, Figure S3: Excitation spectra of compounds monitored at the emission maxima: (a) λ_{em} = 381 nm for **1** and (b) λ_{em} = 391 nm for **2**, **Figure S4**: Comparative view of the absorption spectra of compounds (a) **1** and (b) **2** in solid state and aqueous solution, Figure S5: The most representative intermolecular interactions and packing modes for complexes **1** (up) and **2** (down). H bonds, π···π and C–H···π interactions are shown with dashed blue, green and orange lines, respectively, Figure S6: View along a (left), b (middle) and c (right) axis of complex **1** (up) and **2** (down), Figure S7: UV-Vis spectra of compounds (a) **1** and (b) **2** in aqueous solutions acquired at times (0 h and after 24 h), Table S1: Selected bond lengths (Å) and angles (°) for complexes **1** and **2**, Table S2: Continuous Shape Measurements for the ZnN_2O_2 coordination environment, Table S3: Continuous Shape Measurements for the CdN_2O_4 coordination environment. The CIF and the checkCIF output files are included in the Supplementary Materials.

Author Contributions: Conceptualization, A.R.-D.; methodology, A.A.G.-V. and E.E.-E.; software, J.C.; validation, J.M.D.-L. and S.R.; formal analysis, B.F. and S.R.; investigation, A.A.G.-V. and G.B.R.-R.; resources, B.F. and A.R.-D.; data curation, G.B.R.-R. and J.C.; writing—original draft preparation, E.E.-E.; writing—review and editing, J.C. and A.R.-D.; visualization, B.F.; supervision, A.R.-D.; project administration, J.C. and A.R.-D.; funding acquisition J.C. and A.R.-D. All authors have read and agreed to the published version of the manuscript.

Funding: Financial support was given by Junta de Andalucía (Spain) (FQM-394), University of the Basque Country (GIU 17/13), Gobierno Vasco/Eusko Jaurlaritza (IT1005-16), and the Spanish Ministry of Science, Innovation and Universities (MCIU/AEI/FEDER, UE) (PGC2018-102052-A-C22, PGC2018-102052-B-C21). J.M.D.L. and G.B.R.R. acknowledge the FEDER/MCIU/AEI for their Ramón y Cajal (RYC-2016-21042) and Juan de la Cierva (JdC-2017) fellowships, respectively. S.R. acknowledges the Juan de la Cierva Incorporación Fellowship (grant agreement nº. IJC2019-038894-I). E.E.-E. is grateful to the Government of the Basque Country for the predoctoral fellowship. The authors thank for technical and human support provided by SGIker of UPV/EHU and European funding (ERDF and ESF).

Institutional Review Board Statement: Not applicable.

Informed Consent Statement: Not applicable.

Conflicts of Interest: The authors declare no conflict of interest.

References

1. McKinlay, A.C.; Morris, R.E.; Horcajada, P.; Férey, G.; Gref, R.; Couvreur, P.; Serre, C. BioMOFs: Metal-organic frameworks for biological and medical applications. *Angew. Chem. Int. Ed.* **2010**, *49*, 6260–6266. [CrossRef]
2. Tranchemontagne, D.J.; Tranchemontagne, J.L.; O'keeffe, M.; Yaghi, O.M. Secondary building units, nets and bonding in the chemistry of metal–organic frameworks. *Chem. Soc. Rev.* **2009**, *38*, 1257–1283. [CrossRef] [PubMed]
3. Zhang, Q.; Cui, Y.; Qian, G. Goal-directed design of metal–organic frameworks for liquid-phase adsorption and separation. *Coord. Chem. Rev.* **2019**, *378*, 310–332. [CrossRef]
4. Bünzli, J.-C.G. On the design of highly luminescent lanthanide complexes. *Coord. Chem. Rev.* **2015**, *293–294*, 19–47. [CrossRef]
5. Chen, C.T.; Suslick, K.S. One-dimensional coordination polymers: Applications to material science. *Coord. Chem. Rev.* **1993**, *128*, 293–322. [CrossRef]
6. Heravi, M.M.; Zadsirjan, V. Prescribed drugs containing nitrogen heterocycles: An overview. *RSC Adv.* **2020**, *10*, 44247–44311. [CrossRef]
7. Horton, D.A.; Bourne, G.T.; Smythe, M.L. The combinatorial synthesis of bicyclic privileged structures or privileged substructures. *Chem. Rev.* **2003**, *103*, 893–930. [CrossRef]
8. Zhang, S.G.; Liang, C.G.; Zhang, W.H. Recent advances in indazole-containing derivatives: Synthesis and biological perspectives. *Molecules* **2018**, *23*, 2783. [CrossRef]
9. Dong, J.; Zhang, Q.; Wang, Z.; Huang, G.; Li, S. Recent Advances in the Development of Indazole-based Anticancer Agents. *ChemMedChem* **2018**, *13*, 1490–1507. [CrossRef]
10. Büchel, G.E.; Kossatz, S.; Sadique, A.; Rapta, P.; Zalibera, M.; Bucinsky, L.; Komorovsky, S.; Telser, J.; Eppinger, J.; Reiner, T.; et al. Cis -Tetrachlorido-bis(indazole)osmium(IV) and its osmium(III) analogues: Paving the way towards the cis -isomer of the ruthenium anticancer drugs KP1019 and/or NKP1339. *Dalt. Trans.* **2017**, *46*, 11925–11941. [CrossRef]
11. Hawes, C.S.; Kruger, P.E. Discrete and polymeric Cu(ii) complexes featuring substituted indazole ligands: Their synthesis and structural chemistry. *Dalt. Trans.* **2014**, *43*, 16450–16458. [CrossRef]

12. Long, B.F.; Huang, Q.; Wang, S.L.; Mi, Y.; Wang, M.F.; Xiong, T.; Zhang, S.C.; Yin, X.H.; Hu, F.L. Five new cobalt(II) complexes based on indazole derivatives: Synthesis, DNA binding and molecular docking study. *J. Coord. Chem.* **2019**, *72*, 645–663. [CrossRef]
13. Furman, J.D.; Burwood, R.P.; Tang, M.; Mikhailovsky, A.A.; Cheetham, A.K. Understanding ligand-centred photoluminescence through flexibility and bonding of anthraquinone inorganic-organic frameworks. *J. Mater. Chem.* **2011**, *21*, 6595–6601. [CrossRef]
14. Yuan, W.Z.; Shen, X.Y.; Zhao, H.; Lam, J.W.Y.; Tang, L.; Lu, P.; Wang, C.; Liu, Y.; Wang, Z.; Zheng, Q.; et al. Crystallization-induced phosphorescence of pure organic luminogens at room temperature. *J. Phys. Chem. C* **2010**, *114*, 6090–6099. [CrossRef]
15. Cepeda, J.; Rodríguez-Diéguez, A. Tuning the luminescence performance of metal-organic frameworks based on d10metal ions: From an inherent versatile behaviour to their response to external stimuli. *CrystEngComm* **2016**, *18*, 8556–8573. [CrossRef]
16. Solov'ev, K.N.; Borisevich, E.A. Intramolecular heavy-atom effect in the photophysics of organic molecules. *Phys. Uspekhi* **2005**, *48*, 231–253. [CrossRef]
17. Seco, J.M.; Pérez-Yáñez, S.; Briones, D.; García, J.Á.; Cepeda, J.; Rodríguez-Diéguez, A. Combining Polycarboxylate and Bipyridyl-like Ligands in the Design of Luminescent Zinc and Cadmium Based Metal-Organic Frameworks. *Cryst. Growth Des.* **2017**, *17*, 3893–3906. [CrossRef]
18. Cepeda, J.; Pérez-Yáñez, S.; Rodríguez-Diéguez, A. Luminescent Zn/Cd-based MOFS, CPS and their applications. In *Advances in Materials Science Research*; Wythers, M.C., Ed.; Nova Science Publishers: Hauppauge, NY, USA, 2017; Volume 28, ISBN 9781536109054.
19. San Sebastian, E.; Rodríguez-Diéguez, A.; Seco, J.M.; Cepeda, J. Coordination Polymers with Intriguing Photoluminescence Behavior: The Promising Avenue for Greatest Long-Lasting Phosphors. *Eur. J. Inorg. Chem.* **2018**, 2155–2174. [CrossRef]
20. Pajuelo-Corral, O.; Rodríguez-Diéguez, A.; García, J.A.; San Sebastián, E.; Seco, J.M.; Cepeda, J. Chiral coordination polymers based on d10metals and 2-aminonicotinate with blue fluorescent/green phosphorescent anisotropic emissions. *Dalt. Trans.* **2018**, *47*, 8746–8754. [CrossRef]
21. Yang, Y.; Wang, K.Z.; Yan, D. Ultralong Persistent Room Temperature Phosphorescence of Metal Coordination Polymers Exhibiting Reversible pH-Responsive Emission. *ACS Appl. Mater. Interfaces* **2016**, *8*, 15489–15496. [CrossRef]
22. Liu, Q.; Wang, R.; Wang, S. Blue phosphorescent Zn(II) and orange phosphorescent Pt(II) complexes of 4,4′-diphenyl-6,6′-dimethyl-2,2′-bipyrimidine. *Dalt. Trans.* **2004**, *35*, 2073–2079. [CrossRef]
23. Barbieri, A.; Accorsi, G.; Armaroli, N. Luminescent complexes beyond the platinum group: The d10 avenue. *Chem. Commun.* **2008**, 2185–2193. [CrossRef]
24. Hu, Z.; Deibert, B.J.; Li, J. Luminescent metal-organic frameworks for chemical sensing and explosive detection. *Chem. Soc. Rev.* **2014**, *43*, 5815–5840. [CrossRef] [PubMed]
25. Leo, P.; Briones, D.; García, J.A.; Cepeda, J.; Orcajo, G.; Calleja, G.; Rodríguez-Diéguez, A.; Martínez, F. Strontium-Based MOFs Showing Dual Emission: Luminescence Thermometers and Toluene Sensors. *Inorg. Chem.* **2020**, *59*, 18432–18443. [CrossRef]
26. Liu, J.; Zhuang, Y.; Wang, L.; Zhou, T.; Hirosaki, N.; Xie, R.-J. Achieving Multicolor Long-Lived Luminescence in Dye-Encapsulated Metal–Organic Frameworks and Its Application to Anticounterfeiting Stamps. *ACS Appl. Mater. Interfaces* **2018**, *10*, 1802–1809. [CrossRef]
27. Sun, Y.-X.; Sun, W.-Y. Zinc(ii)– and cadmium(ii)–organic frameworks with 1-imidazole-containing and 1-imidazole-carboxylate ligands. *CrystEngComm* **2015**, *17*, 4045–4063. [CrossRef]
28. Alvarez, S.; Avnir, D.; Llunell, M.; Pinsky, M. Continuous symmetry maps and shape classification. The case of six-coordinated metal compounds. *New J. Chem.* **2002**, *26*, 996–1009. [CrossRef]
29. Volkringer, C.; Loiseau, T.; Guillou, N.; Fèrey, G.; Haouas, M.; Taulelle, F.; Audebrand, N.; Margiolaki, I.; Popov, D.; Burghammer, M.; et al. Structural transitions and flexibility during dehydration—Rehydration process in the MOF-type aluminum pyromellitate A12(OH)2[C1008H2](MIL-118). *Cryst. Growth Des.* **2009**, *9*, 2927–2936. [CrossRef]
30. Boča, M.; Baran, P.; Boča, R.; Fuess, H.; Kickelbick, G.; Linert, W.; Renz, F.; Svoboda, I. Selective imidazolidine ring opening during complex formation of iron(III), copper(II), and zinc(II) with a multidentate ligand obtained from 2-pyridinecarboxaldehyde N-oxide and triethylenetetramine. *Inorg. Chem.* **2000**, *39*, 3205–3212. [CrossRef]
31. Xiao, H.; Li, X.B.; Qin, G.F.; Xia, Y.; Zhou, G. Directed assembly of cobalt(II) 1-H-indazole-3-carboxylic acid coordination networks by bipyridine and its derivatives: Structural versatility, electrochemical properties, and antifungal activity. *J. Iran. Chem. Soc.* **2016**, *13*, 793–802. [CrossRef]
32. Ohno, K.; Okimura, M.; Akai, N.; Katsumoto, Y. The effect of cooperative hydrogen bonding on the OH stretching-band shift for water clusters studied by matrix-isolation infrared spectroscopy and density functional theory. *Phys. Chem. Chem. Phys.* **2005**, *7*, 3005–3014. [CrossRef] [PubMed]
33. Salinas-Castillo, A.; Calahorro, A.J.; Briones, D.; Fairen-Jiménez, D.; Gándara, F.; Mendicute-Fierro, C.; Seco, J.M.; Pérez-Mendoza, M.; Fernández, B.; Rodríguez-Diéguez, A. 2D-cadmium MOF and gismondine-like zinc coordination network based on the N-(2-tetrazolethyl)-4′-glycine linker. *New J. Chem.* **2015**, *39*, 3982–3986. [CrossRef]
34. Pamei, M.; Puzari, A. Luminescent transition metal–organic frameworks: An emerging sensor for detecting biologically essential metal ions. *Nano-Struct. Nano-Objects* **2019**, *19*, 100364. [CrossRef]
35. García-Valdivia, A.A.; Zabala-Lekuona, A.; Ramírez-Rodríguez, G.B.; Delgado-López, J.M.; Fernández, B.; Cepeda, J.; Rodríguez-Diéguez, A. 2D-Coordination polymers based on 1H-indazole-4-carboxylic acid and transition metal ions: Magnetic{,} luminescence and biological properties. *CrystEngComm* **2020**, *22*, 5086–5095. [CrossRef]

36. García-Valdivia, A.A.; Pérez-Mendoza, M.; Choquesillo-Lazarte, D.; Cepeda, J.; Fernández, B.; Souto, M.; González-Tejero, M.; García, J.A.; Espallargas, G.M.; Rodríguez-Diéguez, A. Interpenetrated Luminescent Metal–Organic Frameworks based on 1H-Indazole-5-carboxylic Acid. *Cryst. Growth Des.* **2020**, *20*, 4550–4560. [CrossRef]
37. Dobretsov, G.E.; Syrejschikova, T.I.; Smolina, N.V. On mechanisms of fluorescence quenching by water. *Biophysics* **2014**, *59*, 183–188. [CrossRef]
38. Bruker Apex2. *B.A.I. Bruker Apex2*; Bruker AXS Inc.: Madison, WI, USA, 2004.
39. Sheldrick, G.M. SADABS 1996, Program for Empirical Adsorption Correction. Available online: https://cmacd.myweb.cs.uwindsor.ca/Teaching/553-class/sadabs.pdf (accessed on 16 January 2021).
40. Sheldrick, G.M. SHELXT—Integrated space-group and crystal-structure determination. *Acta Crystallogr. Sect. A Found. Crystallogr.* **2015**, *71*, 3–8. [CrossRef]